AAPM 48th Annual Meeting
July 30 - August 3, 2006
Orange County Convention Center
Orlando, FL

Washington University in St.Louis School of Medicine
MIR Mallinckrodt Institute of Radiology

Stochastic Noise in CT Images

Bruce R. Whiting[1], Parinaz Massoumzadeh[1], Donald L. Snyder[1], Jeffrey F. Williamson[2]

(1) Mallinckrodt Institute of Radiology, Washington University, St. Louis, MO

(2)Virginia Commonwealth University, Richmond, VA

VCU Health System
MCV Hospitals and Physicians

AAPM 48th Annual Meeting
July 30 - August 3, 2006
Orange County Convention Center
Orlando, FL

▶ 1. Introduction

Development of CT protocols that minimize radiation dose for specific clinical tasks is an active area of investigation, involving the tradeoff between radiation dose and image quality. The relative complex texture of CT noise, which is non-local and anisotropic (Figure 1), and the difficulty of measuring stochastic noise in the presence of anatomical structure complicate this research.

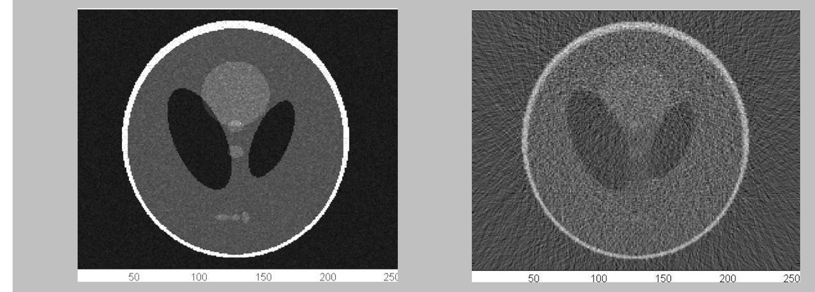

Figure 1- The same phantom image slice was generated with a conventional x-ray process (left) and a CT process (right), in the presence of transmission-domain Poisson noise. Note the difference in texture and distribution of the noise appearance.

Image variance mapping is a venerable tool[1] that recently has been proposed[2] for predicting image noise properties. This poster examines its application and limitations under clinical conditions.

▶ 2. Methods

Noise properties of CT images must be studied beginning with raw projection measurements (sinograms), defined as[3]:

$$A_m(D,\Theta,z') = \log\left(\frac{S_0(D,\Theta,z')}{S_m(D,\Theta,z')}\right),$$

where S_i is the measured or reference flux, and the argument variables are detector, gantry, and table position. Image reconstruction is a linear process, mapping projections into images through signal-processing steps such as interpolation, filtering, and back projection. These

▶ 2. Methods (continued)

can be combined and represented as a linear operator for image formation

$$I(x,y,z) = \sum_{z'}\sum_{\Theta}\sum_{D} K_{x,y,z,D,\Theta,z'} A(D,\Theta,z').$$

Under certain conditions, image variance σ_I^2 can be predicted by the expression:

$$\sigma_I^2(x,y,z) = \sum_{z'}\sum_{\Theta}\sum_{D} K^2_{x,y,z,D,\Theta,z'} \sigma_A^2(D,\Theta,z')$$

In the following, the factors contributing to CT variance will be explained, and the results of the analysis will be compared to simulations.

▶ 2a. Sinogram Variance

CT scanners measure the x-ray flux transmitted through objects, and have noise properties obeying Compound Poisson statistics[4]. For clinical conditions, the variance of the measurements is essentially proportional to the mean of the signal. Given that the sinograms consist of the logarithm of the measured flux, a commonly used approximation[1,5] for the variance of the logarithmic variable is

$$\sigma_A^2 \approx \left(\frac{\partial \ln\left(S_0/S\right)}{\partial S}\right)^2 \sigma_S^2 = \left(1/S\right)^2 S = 1/S = e^A/S_0$$

However, this approximation relies on the fact that the measurement fluctuations must be much less than the mean measured value[6], *(S+ds)/S-1<<1*, so *log(1+x)~x*, otherwise significant errors can result. The validity of these approximations for a Poisson process are shown in Figure 2, indicating the range of signals where the approximation holds. At low signal levels,

▶ 2a. Sinogram Variance (continued)

far below typical clinical protocols, the noise (and mean) will be overestimated by this approximation.

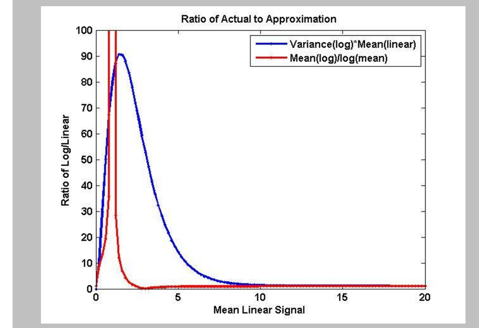

Fig. 2- Accuracy of the log approximation for a simple Poisson distribution. The mean and variance of the log(S) (with log(S=0) fixed at 14, typical of CT data storage) are divided by the log(mean) and variance of a Poisson. For means <10, the approximation performs poorly.

Because modern CT scanners designs have features to minimize patient dose, the flux level of an individual measurement varies due to bowtie filters and tube current modulation (Figure 3).

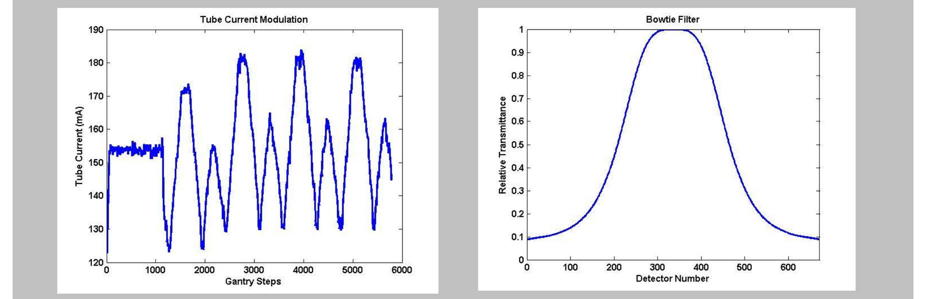

Figure 3- The intensity of individual detectors will vary due to tube current modulation (left) and the bowtie filter (right).

▶ 2b. Interpolation and filtering

Interpolation is performed in several stages of the image reconstruction process, e.g., converting from a fan-beam to fan-parallel geometry, interpolating from helical to planar sections, or backprojecting filtered sinograms into the image domain. Often linear interpolation schemes are used, e.g.,

$$Y = wX_1 + (1-w)X_2; \quad \sigma_Y^2 = w^2\sigma_{X_1}^2 + (1-w)^2\sigma_{X_2}^2.$$

Filtered backprojection utilizes a ramp frequency filter, which corresponds to convolution with a 1D kernel. In the variance term, the coefficients of the linear kernel are squared, corresponding

▶ 2b. Interpolation and filtering (continued)

to a convolution in the frequency domain. Thus the variance sinogram must be properly filtered before backprojection.

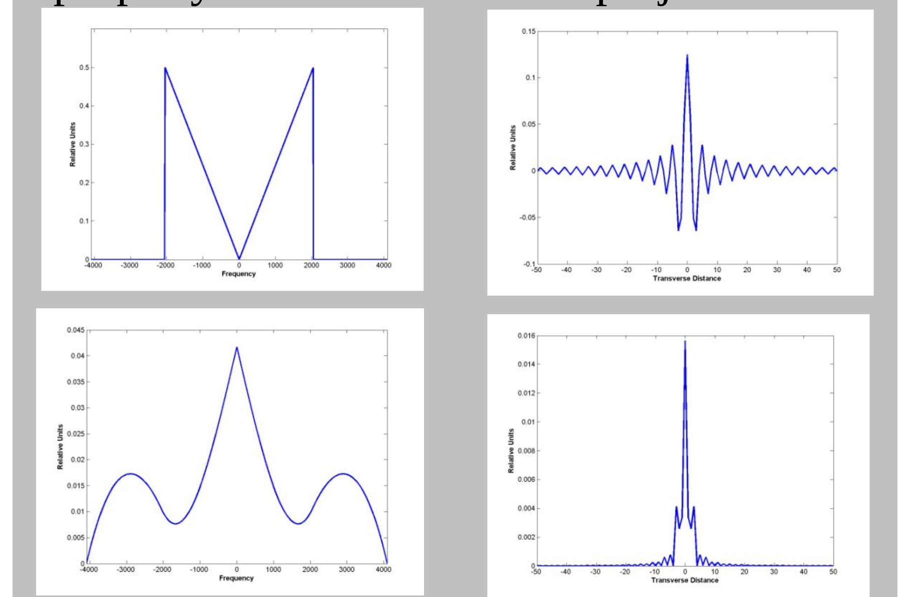

Figure 4- Top left- windowed ramp filter; top right- reconstruction kernel; bottom right- square of reconstruction kernel for weighting sinogram variance; bottom left- Fourier transform of variance kernel (formed by convolution of the ramp filter).

▶ 2c. Simulation

Simulated images were created by exponentiating attenuation sinograms (including the bowtie filter and tube modulation) and scaling to a mean flux level. This was passed through a Poisson random-noise generator, and then converted back into attenuation. Sinograms were reconstructed using offline software.

▶ 3. Results

Sinograms of a 35 cm cylinder were used as input to a variance mapping. A series of 25 images were created from sinograms with simulated random noise and analyzed for

▶ 3. Results (continued)

mean and variance. Figure 5a shows a comparison of the relative noise distribution predicted by noise mapping versus measurements of the simulations, demonstrating excellent agreement. Figure 5b shows the effect of the bowtie filter on noise distributions. Figure 6 demonstrates the influence of flux level on estimates of image mean and variance. As predicted in Figure 2, for fluxes >10, the mean and relative variance are independent of flux, while for low-flux conditions the mean and variance are overestimated. Variance mapping can be used to analyze noise in clinical images, as shown in Figure 7.

▶ 4. Conclusions

The range of validity for image variance mapping was predicted and verified by simulations. For common clinical scan conditions, image variance mapping is a useful tool for studying the effects of CT noise on image quality and developing protocols for radiation dose reduction.

▶ 5. References

1-Chesler, D.A., S.J. Riederer and N.J. Pelc, *Noise due to photon counting statistics in computed X-ray tomography.* J Comput Assist Tomogr, 1977. **1**(1): p. 64-74.

2- Kachelrieß, M. *Refresher Course RC 1213: Image quality and dose in multislice CT: Current practice, new developments and optimization A. Basic considerations (A-278)*. in *ECR 2004*. 2004. Vienna, Austria.

3- Kak, A. and M. Slaney (1988). Principles of Computerized Tomography, IEEE Press.

4. Whiting, BR, et. al, *Properties of preprocessed sinogram data in X-ray computed tomography*, Med Phys, 2006, IN PRESS

5. Gies, M., et al., *Dose reduction in CT by anatomically adapted tube current modulation. I. Simulation studies*. Med Phys, 1999. **26**(11): p. 2235-47

6. Papoulis, A. and U. Pillai, Probability, Random Variables and Stochastic Processes Fourth Edition, McGraw Hill, New York (2002), page 215

▶ 3. Results (continued)

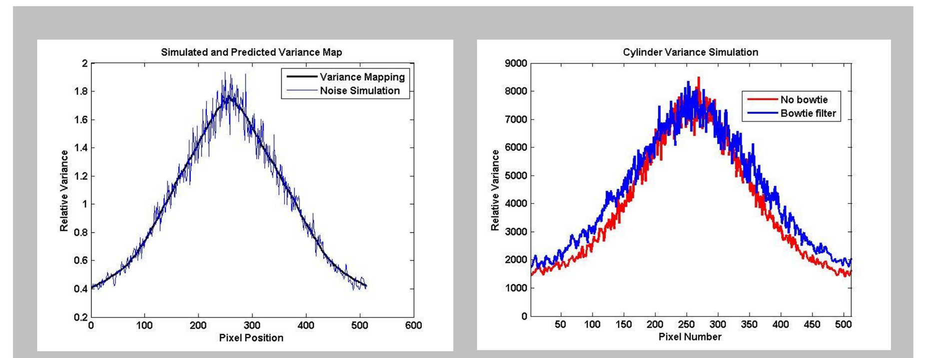

Figure 5. a) Plot of variance along the cylinder diameter for variance mapping and simulation (mean variance for 25 simulations); b) Simulations with and without a bowtie present- the bowtie filter increases edge noise.

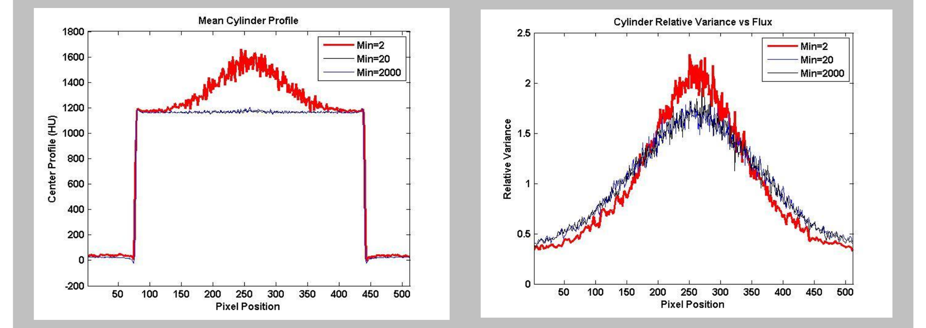

Figure 6. a) Plot of mean profile through cylinder center as a function of flux level. For higher flux (where the minimum mean is 20 or greater), flat profile is seen; for low flux regions (means ~2), attenuation is overestimated; b) Plot of variance, indicating that variance is overestimated for low-flux conditions.

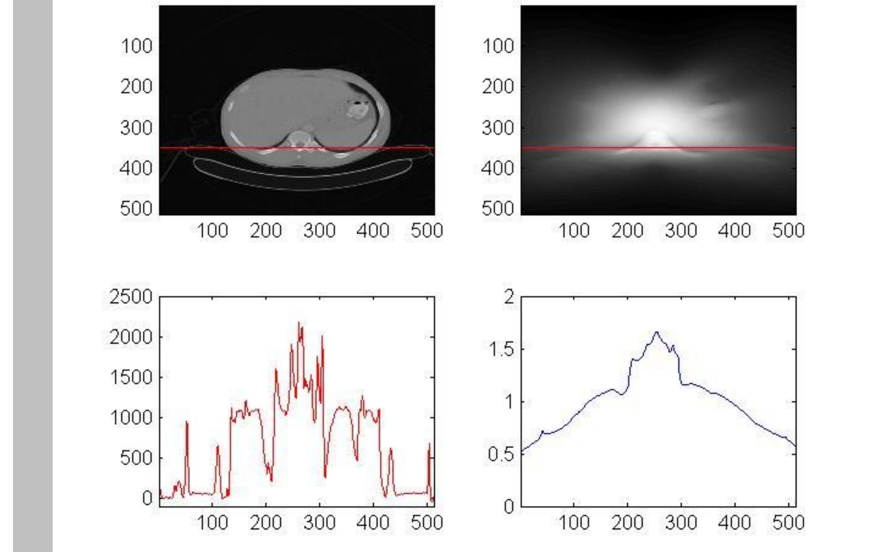

Figure 7. Top left, reconstructed image; bottom left, profile through red line in reconstructed image; top right, noise variance map; bottom right, profile of relative variance map through red line. Note that in the image profile there are rapidly changing attenuation levels, whereas the variance changes slowly over extended distances.

▶6. Acknowledgements

Financial support for this research was provided by the Electronic Radiology Lab of the Mallinckrodt Institute of Radiology, and NIH grants (NIH/NCI R21 CA95408 (PI BR Whiting) and 2R01CA075371-05A1 (PI: JF Williamson). Siemens Medical Solutions provided reconstruction software. David G. Politte, D.Sc., provided reconstruction kernel plots.